ISSN 1062-8738, Bulletin of the Russian Academy of Sciences: Physics, 2021, Vol. 85, No. 2, pp. 201–205. © Allerton Press, Inc., 2021.
Russian Text © The Author(s), 2021, published in Izvestiya Rossiiskoi Akademii Nauk, Seriya Fizicheskaya, 2021, Vol. 85, No. 2, pp. 276–281.

Using Holographic Interferometry to Transmit Information through a Perturbed Ocean Environment

V. M. Kuz'kin[a], M. Badiey[b], S. A. Pereselkov[c, *], and E. S. Kaznacheeva[c]

[a] *Prokhorov General Physics Institute, Russian Academy of Sciences, Moscow, 119991 Russia*
[b] *University of Delaware, Newark, DE 19716 USA*
[c] *Voronezh State University, Voronezh, 394006 Russia*
**e-mail: pereselkov@yandex.ru*

Received August 28, 2020; revised September 25, 2020; accepted October 28, 2020

Abstract—The theory of interferometric processing of hydroacoustic information is generalized to when intense nonlinear internal waves result in coupling of the sound field modes. A theoretical explanation is given for experimental data on the forming of a hologram in the presence of intense nonlinear internal waves. The error in transmitting unperturbed information through a perturbed ocean environment is estimated.

DOI: 10.3103/S1062873821020179

INTRODUCTION

Interferometric processing [1–3] is based on coherent accumulation of the spectral intensity of the wave field along localized bands of the interference pattern (interferogram) in frequency–time variables, which is formed by a broadband source and further subjected to a double Fourier transform. As a result of an integral transform, the spectral density is concentrated within a narrow band in the form of focal spots caused by interference between modes of different numbers. In contrast to the signal, the accumulation of noise along the interferogram bands is noncoherent and distributed over the domain of the double integral transform. The noisy interferogram is reconstructed by filtering the two-dimensional spectral density of the signal with a subsequent inverse double Fourier transform applied to it. The transformed spectral density of the interferogram is referred to as a hologram, and the processing itself is referred to as holographic interferometry, allowing us to select weak signals against the background of intense noise. The regular interference pattern from such processing is caused by waveguide dispersion and the multimode propagation of sound waves.

The most obvious application of holographic interferometry is the localization of low-noise sources [1–3]. Two adaptive algorithms of interferometric processing were developed on its basis, solving the problem of localizing low-noise sources under the conditions of no a priori information on the transfer function of ocean environment [4–6].

Another valuable application of holographic interferometry is due to the possibility of transmitting undistorted hydroacoustic information through a randomly inhomogeneous ocean environment. This effect was first observed experimentally in the SWARM-95 experiment [7, 8] from the propagation of a broadband signal on a stationary path perturbed by intense internal waves (IIWs). It was described in [9, 10].

Based on a theoretical analysis and numerical modeling, in this work we study the mechanism of interferogram and hologram formation when IIWs result in coupling of the sound field modes. The experimental formation of two non-overlapping hologram domains [10] is explained as being determined by unperturbed and diffused fields. The error in reconstructing the unperturbed field interferogram is estimated.

FORMATION OF A HOLOGRAM IN THE PRESENCE OF IIWs

Theoretical validation of the possibility of avoiding distortions of data in the presence of hydrodynamic perturbations is based on presenting an interferogram as a linear superpositioning of two independent ones generated by unperturbed and diffused fields. Two non-overlapping localized spectral domains then form in the hologram. according to the linearity of a double inverse Fourier transform. One is caused by the unperturbed field and is concentrated in the form of focal spots preferentially toward the time axis; the second is due to hydrodynamic perturbations and directed along the frequency axis. Filtering these domains allows us to resolve holograms of the unperturbed and diffused fields. Applying a double inverse Fourier transform to them lets us reconstruct interferograms of those fields.

One of these is determined by the interference of modes of the unperturbed environment; the other forms due to the environment's variability.

With coupled modes, variations in the refraction index induce an exchange of energy between the complex amplitudes of modes. Variations in the phase determining the pattern of the localized interferogram bands are due to one in both the horizontal wavenumbers and mode amplitudes. Phase corrections with respect to the unperturbed value can be determined from small perturbations, allowing us to describe the weak intermode transformation typical of ocean inhomogeneities.

For simplicity, we limit ourselves to considering IIWs in the form of a single soliton propagating along an acoustic path. The corrections to complex amplitudes A_m are determined using a system of linear differential first-order equations for coupled modes:

$$\frac{dA_m(x,t)}{dx} = i\sum_n \{\xi_m \delta_{mn} + \mu_{mn}(x,t)\} A_n(x,t), \quad (1)$$

where $\xi_m = h_m + i\gamma_m$ is the complex horizontal wavenumber of the mth mode, δ_{mn} is the Kronecker delta, x is the current horizontal distance between the source and receiver, and t is time [11]. Unperturbed quantities are indicated by the numerator; perturbed quantities, by the denominator.

The coefficients of mode coupling are equal to

$$\mu_{mn}(x,t) = \frac{\bar{k}_0^2}{2\sqrt{\bar{h}_m \bar{h}_n}} \int_0^H \bar{\psi}_m(z)\bar{\psi}_n(z)\tilde{n}^2(x,z,t)\,dz. \quad (2)$$

Here, $\bar{k}_0^2$ is the square of the wavenumber at depth $z = 0$, and $\bar{\psi}_m(z)$ is the eigenfunction of the mth mode. The perturbed component of the refraction index is written as

$$\tilde{n}^2(x,z,t) = -2QN^2(z)\Phi(z)\zeta(x,t), \quad (3)$$

where $Q \approx 2.4$ s^2/m is a constant determined by physical properties of water, $N(z)$ is the buoyancy frequency, $\Phi(z)$ is the eigenfunction of the first gravitational mode normalized by the eigenvalue at the depth of detection, and H is the depth of the waveguide [12]. Vertical displacements of water layers $\zeta(x,t)$, determined by the solution to the Korteweg–de Vries equation, are

$$\zeta(x,t) = -B\,\mathrm{sech}^2[(x-ut)/\eta]. \quad (4)$$

Here, B and η are the soliton amplitude and half-width at the level of 0.42 of the maximum, and u is the speed of propagation.

Considering the smallness of $\tilde{n}^2$ with respect to $\bar{n}^2$, $\tilde{n}^2 \ll \bar{n}^2$, resulting field p is written as

$$p = p_0 + p_s, \quad (5)$$

where p_0 is an unperturbed field that satisfies wave equation

$$\Delta p(x,z,t) + \bar{k}_0^2\left(\bar{n}^2(z) + \tilde{n}^2(x,z,t)\right)p(x,z,t) = 0 \quad (6)$$

with corresponding boundary conditions at $\tilde{n}^2(x,z,t) = 0$, and p_s is a diffuse field of the first order with respect to $\tilde{n}^2$. We write fields $p_{0,s}$ as the sum of the modes

$$p_0(\omega) = \sum_m \bar{A}_m(\omega)\exp(i\bar{h}_m(\omega)x_0), \quad (7)$$

$$p_s(\omega,t) = \sum_m \tilde{A}_m(\omega,t)\exp(i\Phi_m(\omega,t)), \quad 0 \le x(t) \le x_0. \quad (8)$$

Here, $\Phi_m(\omega,t) = \int_0^{x(t)} \tilde{h}_m(\omega,t)\,dx'$ is the phase of the mth mode of the diffuse field, and x_0 is the distance between the source and receiver. Adjustments $\tilde{A}_m$ and $\tilde{h}_m$ are determined from the solution to the system of Eqs. (1). The cylindrical divergence of the field, the attenuation of modes, and depths z_s and z_q of the source and receiver are formally considered in the dependence of the mode amplitudes.

According to (5), the interferogram of the resulting field $I = |p|^2$ is equal to

$$I = p_0 p_0^* + p_s p_0^* + p_0 p_s^* + p_s p_s^*, \quad (9)$$

where the asterisks indicate complex conjugate quantities. The first and fourth terms are interferograms of the unperturbed and diffused fields, and the second and third terms are interferograms determined by the product of the unperturbed and diffused fields. The unperturbed and diffused fields are not coherent, so the second and third terms can be considered as a background (mean value) that reduces the contrast of the resulting interferogram.

Let us subtract from interferogram I (9) mean value $\bar{\bar{I}}$, $\ddot{I} = I - \bar{\bar{I}}$. Then

$$\ddot{I}(\omega,t) = \ddot{I}_0(\omega) + \ddot{I}_s(\omega,t). \quad (10)$$

According to (7) and (8)

$$\ddot{I}_0(\omega) = \sum_m \sum_n \bar{A}_m(\omega)\bar{A}_n^*(\omega)\exp(i\bar{h}_{mn}(\omega)x_0) = \sum_m \sum_n \ddot{I}_0^{(mn)}(\omega),\ m \ne n, \quad (11)$$

$$\ddot{I}_s(\omega,t)\sum_m \sum_n \tilde{A}_m(\omega,x(t),t)\tilde{A}_n^*(\omega,x(t),t) \times \exp\left(i\int_0^{x(t)} \tilde{h}_{mn}(\omega,t)\,dx'\right) = \sum_m \sum_n \ddot{I}_s^{(mn)}(\omega,t),\quad m \ne n. \quad (12)$$

Here, $\bar{h}_{mn} = \bar{h}_m - \bar{h}_n$, $\tilde{h}_{mn} = \tilde{h}_m - \tilde{h}_n$. When there is perturbation, the interferogram is the sum of interferograms of the unperturbed and diffused fields.

Let us apply double Fourier transform to interferogram $\ddot{I}(\omega,t)$ (10). We then obtain the sum of holograms of unperturbed and diffuse fields:

$$F\left(\dot{\nu},\tau\right) = \sum_m \sum_n \int_0^{\Delta t} \int_{\omega_1}^{\omega_2} \left[\ddot{I}_0^{(mn)}(\omega) + \ddot{I}_s^{(mn)}(\omega,t)\right] \times \exp\left[i\left(\dot{\nu}\, t - \tau\omega\right)\right] dt d\omega \qquad (13)$$
$$= \sum_m \sum_n F_0^{(mn)}\left(\dot{\nu},\tau\right) + \sum_m \sum_n F_s^{(mn)}\left(\dot{\nu}',\tau\right).$$

Here, $\nu' = 2\pi$ and τ are the circular frequency and period of the hologram; Δt is the period of observation; $\omega_{1,2} = \omega_0 \mp (\Delta\omega/2)$; and $\Delta\omega$ and ω_0 are the width and mean frequency of the spectrum.

Obtaining the hologram of a moving source [1], we acquire a partial hologram of the unperturbed field:

$$F_0^{(mn)}\left(\dot{\nu},\tau\right) = \bar{A}_m(\omega_0)\,\bar{A}_n^*(\omega_0)\,\Delta\omega\Delta t \times \exp\left(i\,\dot{\nu}\,\Delta t/2\right)\exp\left\{i\left[(m-n)\,x_0\alpha - \tau\omega_0\right]\right\} \qquad (14)$$
$$\times \frac{\sin\left(\dfrac{\dot{\nu}\,\Delta t}{2}\right)}{\left(\dfrac{\dot{\nu}\,\Delta t}{2}\right)} \frac{\sin\left[\left((m-n)\,x_0\dfrac{d\alpha}{d\omega} - \tau\right)\dfrac{\Delta\omega}{2}\right]}{\left[\left((m-n)\,x_0\dfrac{d\alpha}{d\omega} - \tau\right)\dfrac{\Delta\omega}{2}\right]},$$

where $\alpha = d\bar{h}_l(\omega_0)/dl = \bar{h}_{l+1}(\omega_0) - \bar{h}_l(\omega_0)$, l is the number of the mode in whose vicinity the modes are in-phase. Introducing value α is useful in interpreting the hologram. In reality, $(d\alpha/d\omega)(m-n) = (d\bar{h}_{mn}(\omega_0)/d\omega)$.

Calculation of the partial hologram of the scattered field (13) can be calculated only numerically. Considering the position of the localization domain of the diffused field on the hologram, however, we can draw some general conclusions even without a numerical solution. Let us assume that in interferogram (12) of a diffuse field, amplitudes $\tilde{A}_{m,n}$ change slowly upon varying the frequency and time, relative to the fast exponential factor. The partial hologram of the diffuse field can then be presented as

$$F_s^{(mn)}(\nu',\tau) = \sum_m \sum_n \tilde{A}_m(\omega_0,t_1)\,\tilde{A}_n^*(\omega_0,t_1) \times \int_0^{\Delta t}\int_{\omega_1}^{\omega_2} \left[\exp\left(i\Phi_{mn}(\omega,t)\right)\exp\left(i\left(\nu' t - \tau\omega\right)\right)\right] dt d\omega. \qquad (15)$$

If the variation in the frequency can be ignored in phase difference $\Phi_{mn}(\omega,t) = \Phi_m(\omega,t) - \Phi_n(\omega,t)$, the spectral density of the diffuse field is concentrated along axis of frequency $\dot{\nu}$. This effect was observed earlier in a field experiment [10]. Otherwise, the spectral density would be localized in a narrow band at an angle to the frequency axis when this dependence must be considered.

With IIWs, two non-overlapped domains of the spectral density of the unperturbed and diffused fields are thus visible on the hologram. Applying an inverse double Fourier transform to the filtered spectral densities allows us to reconstruct two-dimensional holograms of the unperturbed and diffused fields.

NUMERICAL MODELING

We used an unperturbed horizontally homogeneous waveguide similar in characteristics to the experimental channel described in [7, 8]. Two frequency bands were considered: $\Delta f_1 = 100$–120 Hz and $\Delta f_2 = 300$–320 Hz. The characteristics of the fluid absorbing bottom were soil/water density ratio $\rho = 1.8$, complex refraction index $n = 0.84(1 + i0.03)$ for the first frequency band, and $n = 0.84(1 + i0.05)$ for the second band. The distance between the stationary source and receiver $x_0 = 10$ km. The source was located at depth $z_s = 12.5$ m; the receiver at depth $z_q = 35$ m. A uniform spectrum was used: pulses were detected with periodicity of 5 s, and the sampling rate over the frequency of the spectrum of the detected signal was 0.25 Hz. A single soliton moved along the path from the source to receiver. The soliton characteristics were amplitude $B = 15$ m, width $\eta = 150$ m, and speed $w = 0.7$ m/s. The period of observation $\Delta t = 20$ min. The modeling results are presented in Figs. 1–4. To enhance the contrast and information capacity, we omitted the mean values on the interferograms.

Figure 1 shows interferograms and absolute magnitudes of holograms for the unperturbed fields (i.e., when the soliton was beyond the stationary path). Except for the constant factor, the interferogram of the unperturbed field is the waveguide transfer function.

Figure 2 shows the interferograms and absolute magnitudes of holograms for the initial instant of observation, when the soliton is at distance $x_* = 5$ km from the source. In period of observation $\Delta t = 20$ min, the soliton covered distance $\Delta x = 840$ m. At low frequencies corresponding to weak scattering by inhomogeneities, the vertical localized bands typical of the unperturbed waveguide predominate in the final interferogram (Fig. 2a). Raising the frequency increased the scattering, and the contribution from

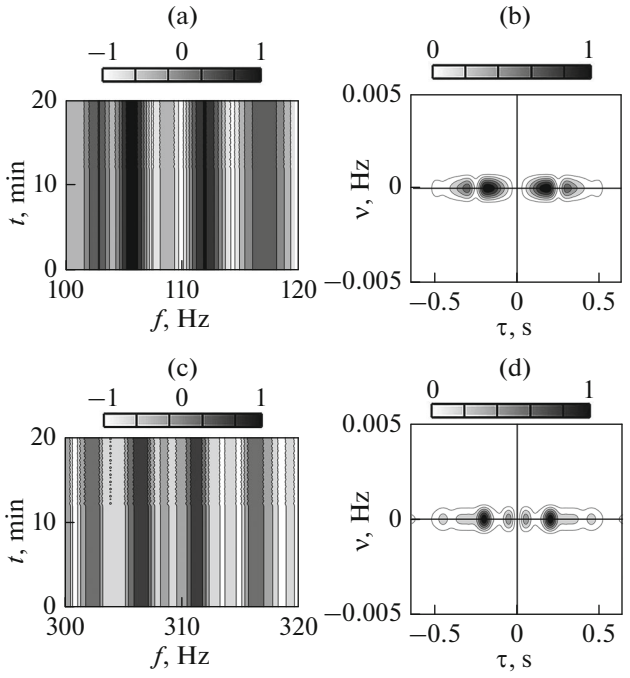

Fig. 1. (a, c) Normalized inteferograms and (b, d) absolute magnitudes of holograms of the unperturbed fields for frequency bands (a, b) Δf_1 and (c, d) Δf_2.

the interference of the scattered field modes resulted in the formation of the horizontal localized bands (Fig. 2c). As a result, the interference pattern became more complicated. In the holograms, the spectral densities of the unperturbed and diffused fields are concentrated in the form of focal spots along the axes of time τ and frequency ν (Figs. 2b, 2d). Beyond those spots, the spectral density is virtually suppressed. The pattern of the focal spots allows us to reconstruct the interferograms of unperturbed and diffused fields.

The results from filtering the spectral densities of the holograms of an unperturbed field localized in the vicinity of the time axes and their Fourier transform are shown in Fig. 3. The interferograms and position mapping of the localized domains on the hologram of the unperturbed field when there is no soliton and the one reconstructed are very similar (see Fig. 1). The position maxima of the focal spots coincide. Their similarity is most clearly seen in Fig. 4.

Figure 4 shows the one-dimensional interferogram of the unperturbed field without the soliton on the path (solid curve) and the reconstructed interferogram (points) with the soliton moving along the path. These are horizontal sections of the two-dimensional inter-

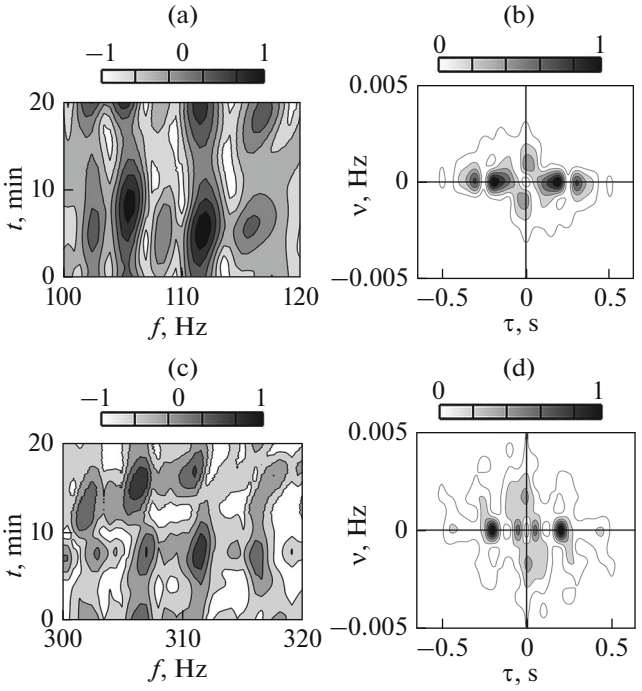

Fig. 2. (a, c) Normalized inteferograms and (b, d) absolute magnitudes of holograms with a soliton on the path for frequency bands (a, b) Δf_1 and (c, d) Δf_2.

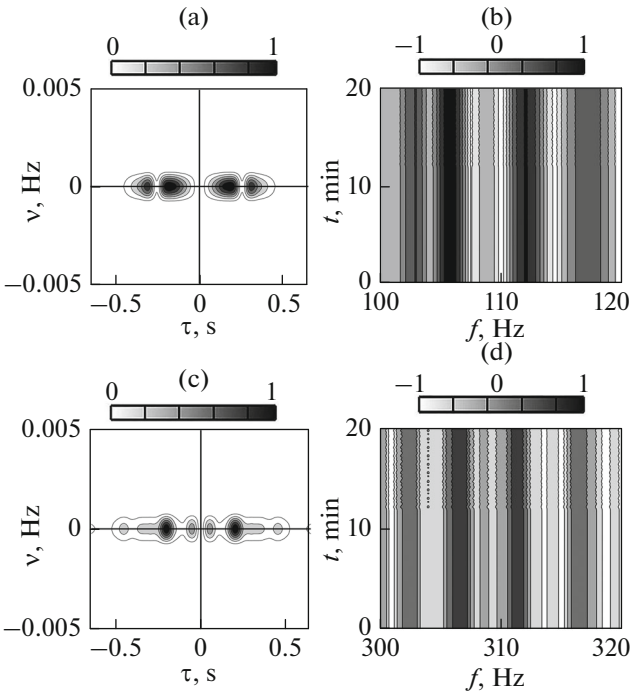

Fig. 3. (a, c) Normalized filtered absolute magnitudes of hologram inteferograms of an unperturbed field and (b, d) interferograms reconstructed from them for frequency bands (a, b) Δf_1 and (c, d) Δf_2.

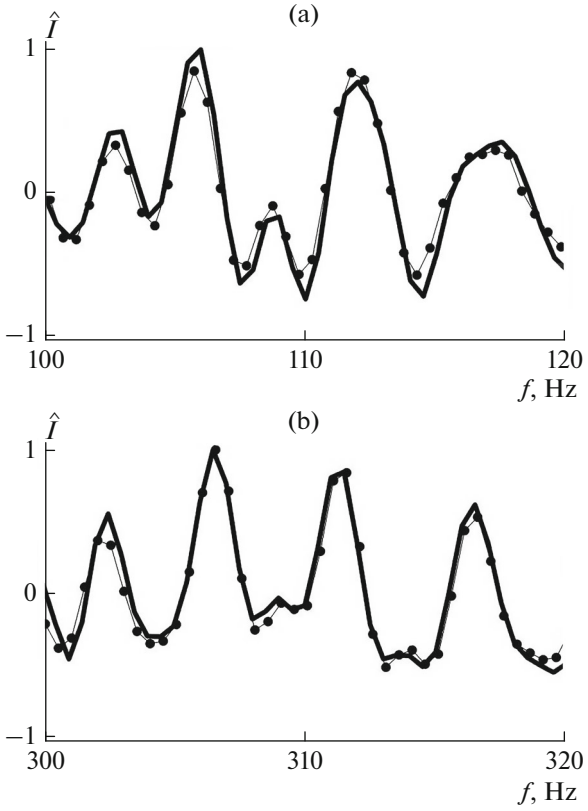

Fig. 4. Frequency dependences of the normalized interferograms of unperturbed fields with no soliton (solid curve) and those reconstructed with solitons (dots).

ferograms (Figs. 1, 3). The error of interferogram reconstruction was estimated as

$$d = \frac{\sum_{j=1}^{J} \left| I_1(f_j) - I_2(f_j) \right|}{\sum_{j=1}^{J} \left| I_1(f_j) \right|}, \qquad (16)$$

where the count number is $J = 80$. Here, $I_{1,2}$ are interferograms of an unperturbed field without a soliton and one reconstructed with one, respectively. For spectral width $\Delta f_1 = 100$–120 Hz, the error is $d = 0.014$; for spectral width $\Delta f_2 = 300$–320 Hz, $d = 0.074$. The difference between errors is determined by the increase in scattering by inhomogeneities as the frequency rises. The normalized values are indicated in Fig. 4 by the caps.

CONCLUSIONS

The possibility of reconstructing the interferogram of an unperturbed field was proved using holographic interferometry under the conditions of coupled modes of the acoustic field of a source caused by a single soliton. Processing was based on the record of the resulting hologram, in the form of non-overlapping localized domains of the spectral densities corresponding to the absence and presence of a perturbation. Reading these domains with an inverse double Fourier transform allowed us to reconstruct the weakly-distorted interferogram of an unperturbed field.

FUNDING

This work was supported by the Russian Foundation for Basic Research, project nos. 19-29-06075 and 19-38-90326. Kaznacheeva E.S. was supported by the grant of the President of the Russian Federation, project no. MK-6144.2021.4.

REFERENCES

1. Kuznetsov, G.N., Kuz'kin, V.M., and Pereselkov, S.A., *Acoust. Phys.*, 2017, vol. 63, no. 4, p. 449.
2. Kuznetsov, G.N., Kuz'kin, V.M., and Pereselkov, S.A., *Bull. Russ. Acad. Sci.: Phys.*, 2017, vol. 81, no. 8, p. 938.
3. Kaznacheev, I.V., Kuznetsov, G.N., Kuz'kin, V.M., and Pereselkov, S.A., *Acoust. Phys.*, 2018, vol. 64, no. 1, p. 37.
4. Kaznacheeva, E.S., Kuznetsov, G.N., Kuz'kin, V.M., et al., *Phys. Wave Phenom.*, 2019, vol. 27, no. 1, p. 73.
5. Kaznacheeva, E.S., Kuz'kin, V.M., Lyakhov, G.A., et al., *Phys. Wave Phenom.*, 2020, vol. 28, no. 3, p. 267.
6. Pereselkov, S.A., Kuz'kin, V.M., and Kuznetsov, G.N., *Bull. Russ. Acad. Sci.: Phys.*, 2020, vol. 84, no. 6, p. 648.
7. Apel, J.R., Badiey, M., Chiu, C.-S., et al., *IEEE J. Ocean. Eng.*, 1997, vol. 22, p. 465.
8. Frank, S.D., Badiey, M., Lynch, J., and Siegmann, W.L., *J. Acoust. Soc. Am.*, 2004, vol. 116, no. 6, p. 3404.
9. Kuz'kin, V.M., Pereselkov, S.A., Zvyagin, V.G., et al., *Phys. Wave Phenom.*, 2018, vol. 26, no. 2, p. 160.
10. Badiey, M., Kuz'kin, V.M., Lyakhov, G.A., et al., *Phys. Wave Phenom.*, 2019, vol. 27, no. 4, p. 313.
11. Katsnel'son, B.G. and Petnikov, V.G., *Akustika melkogo morya* (Shallow Sea Acoustics), Moscow: Nauka, 1997.
12. *Sound Transmission through a Fluctuating Ocean*, Flatté, S.M., Ed., Cambridge: Cambridge Univ. Press, 1979.

Translated by N. Podymova